Journal of Alloys and Compounds 509 (2011) 6236–6241

Contents lists available at ScienceDirect

Journal of Alloys and Compounds

journal homepage: www.elsevier.com/locate/jallcom

A strategy for single-step elaboration of V_2O_5-grafted TiO_2 nanostructured photocatalysts with evenly distributed pores

M.R. Bayati[a,b,*], R. Molaei[b], A.Z. Moshfegh[c,d], F. Golestani-Fard[b,e]

[a] Department of Materials Science and Engineering, North Carolina State University, Raleigh, NC 27695-7907, USA
[b] School of Metallurgy and Materials Engineering, Iran University of Science and Technology, P.O. Box: 16845-161, Tehran, Iran
[c] Department of Physics, Sharif University of Technology, P.O. Box: 11155-9161, Tehran, Iran
[d] Institute for Nanoscience and Nanotechnology, Sharif University of Technology, P.O. Box: 14588-89694, Tehran, Iran
[e] Center of Excellence for Advanced Materials, Iran University of Science and Technology, P.O. Box: 16845-195, Tehran, Iran

ARTICLE INFO

Article history:
Received 15 December 2010
Received in revised form 28 February 2011
Accepted 2 March 2011
Available online 10 March 2011

Keywords:
Micro arc oxidation
Oxide
Surfaces
Catalytic properties

ABSTRACT

V_2O_5–TiO_2 nanostructured porous layers were grown through micro arc oxidation of titanium in vanadate containing electrolytes. This study sheds light on the effect of the electric current type on the photocatalytic performance of the layers. Surface morphology of the layers was investigated by SEM. The results revealed a porous structure with a pores size of 30–180 nm depending on the frequency and the duty cycle. A uniform porous structure was obtained under the pulse-DC regime. Topographical investigations revealed a rough surface which is favorable for catalytic applications. Our XRD and XPS results showed that the layers consisted of anatase, rutile, and vanadium oxide phases whose fraction was observed to change depending on the electric variables. Finally, methylene blue was selected as a model material in order to evaluate the photocatalytic performance of the grown layers. The layers which were fabricated under pulse current, especially those synthesized at the frequency of 500 Hz and duty cycle of 5%, exhibited higher photocatalytic efficiency under ultraviolet and visible illuminations on account of their higher surface area and anatase/rutile fraction.

1. Introduction

Titania (TiO_2) only exhibits its photocatalytic properties under UV illumination due to its relatively wide band gap which is about 3.2 eV. Its wide band gap means that it only absorbs in the UV region of the solar spectrum which represents only 4% of the incoming solar energy. It is necessary to alter TiO_2 surface structure and composition in order to improve its photoactivity under visible irradiation, because UV-irradiation cannot be applied for a long time in practical applications. In addition, its relatively high recombination rate of e^-–h^+ pairs adversely influences the photocatalytic activity [1–4]. Different solutions have been proposed to increase the absorption capacity of TiO_2 under the visible illumination and decrease the e^-–h^+ recombination rate. One of the most important of these solutions is coupling titania with other semiconductors [5–10], metallic, and non-metallic species [11,12]. V_2O_5 is one of the most important metal oxides catalysts with a narrow band gap and its mixture with TiO_2 can be beneficial to improve the photo-catalytic activity. Once optical excitation takes place in the V_2O_5–TiO_2 composite layers, the photo-generated electrons can be transferred to the lower-lying conduction band of V_2O_5, while the positive holes moves toward the valence band of TiO_2 and accumulate there resulting in reduction of the electron-hole recombination rate and consequently photocatalytic activity enhancement. It has also demonstrated that the surface of V_2O_5–TiO_2 layers is more acidic than that of pure TiO_2. The increased acidity can generate a higher affinity of V_2O_5–TiO_2 layers for species with unpaired electrons; therefore, these films could absorb more OH^- or H_2O, and create more OH radical necessary for photo-oxidation reactions. Furthermore, due to the lower band gap energy, the light absorption capacity of the V_2O_5–TiO_2 systems is higher than that of the TiO_2 layers. It results in generation of more e^- and h^+ pairs [13–16]. In addition, V-doping widens the light absorption range of titania and shortens the transition time of electron to the sample surface which is favorable to separate the e^-–h^+ pairs [17].

High quality titania based layers can be obtained via micro arc oxidation (MAO) process [10,18–22]. MAO technology is a relatively new and effective method of fabricating thick, hard, and well-adhered ceramic layers. It is one of the most efficient and simplest methods to grow TiO_2 layers, based on the modification of the growing anodic film by spark arc micro discharges. In this process, the micro discharges rapidly develop and extinguish (within 10^{-4}–10^{-5} s) on the vicinity of the anode and heat the metal substrate to less than 373–423 K. At the same time the local

* Corresponding author. Tel.: +1 919 917 6962; fax: +1 919 515 7724.
E-mail address: mbayati@ncsu.edu (M.R. Bayati).

0925-8388/$ – see front matter © 2011 Elsevier B.V. All rights reserved.
doi:10.1016/j.jallcom.2011.03.013

temperature and pressure inside the discharge channels which are formed by electrical sparks can reach 10^3–10^4 K and 10^2–10^3 MPa, respectively, which are enough to give rise to plasma thermo-chemical interactions between the substrate and the electrolyte. These interactions result in the formation of melt-quenched high-temperature oxides and complex compounds on the surface, composed of oxides of both the substrate material and electrolyte-borne modifying elements. Due to strong electric field (10^6–10^8 V m^{-1}) between anode and cathode, electrolyte anions are drawn into the structural pores where they can attend electrochemical reactions. Structural pores are formed by electron avalanches taking places on the vicinity of the anode. MAO can be expressed as a valid process for "*in situ*" preparing of ceramic coatings. In the case of TiO_2, the phase structure can be controlled by adjusting the experimental conditions [23]. The details of the MAO process can be found elsewhere [24–26].

In our previous study, we employed micro arc oxidation technique and fabricated V_2O_5–TiO_2 layers under direct current. The layers were grown in the electrolytes consisting of sodium phosphate salt with a concentration of 10 g l^{-1} and sodium vanadate salt with concentrations of 1, 2, and 4 g l^{-1} with applying various voltages for 3 min. It was shown that the photocatalytic activity was significantly improved when TiO_2 layers was combined and doped with V_2O_5. Moreover, maximum photocatalytic efficiency was achieved in the layers which were grown under the voltage of 450 V in the electrolytes consisted of sodium vanadate with a concentration of 2 g l^{-1}. It was found that vanadia was partially doped into the titania lattice and dispersed in its matrix as well. We fabricated V_2O_5–TiO_2 layers via MAO process and proposed a formation mechanism for the first [27,28].

In the present study, V_2O_5–TiO_2 porous layers were grown by micro arc oxidation technique under pulse current for the first time. The synthesis conditions were selected based on the obtained results in our previous works [27,29]. Physical and chemical properties of the layers, especially their photocatalytic performance, were compared with those of the layers made under direct current. Hence, we think that it is the first study of its kind.

2. Experimental details

Commercially pure grade II titanium substrates, surrounded by an AISI 316 stainless steel cylindrical container, were used to grow V_2O_5–TiO_2 layers. Details of the surface cleaning procedure as well as schematic illustration of the experimental setup can be found in our previous works [30,31]. The layers were grown in the electrolytes containing sodium phosphate (Merck, 10 g l^{-1}) and sodium vanadate (Merck, 2 g l^{-1}) salts. The treatment time and the applied voltage were same and considered as 3 min and 450 V for all samples, respectively. Meanwhile, frequencies of 250 and 500 Hz and duty cycles of 5 and 25% were applied. Table 1 summarizes all synthesis conditions.

Surface morphology and topography of the layers were examined by scanning electron microscopy (TESCAN, Vega II) and atomic force microscopy (Veeco auto probe) with a silicon tip of 10 nm in radius in contact mode in the atmosphere. X-ray diffraction (Philips, PW3710) and X-ray photoelectron spectroscopy (VG Microtech, Twin anode, XR3E2 X-ray source, equipped with AlKα X-ray source at energy of 1486.6 eV, utilizing hemisphere energy analyzer) techniques were used to study phase structure and chemical composition of the synthesized layers.

Photocatalytic activity of the layers was evaluated by measuring the degradation rate of aqueous methylene blue solution at room temperature. A UV–Vis spectrophotometer (Jasco V-530) was used to measure the change in concentration, based on the Beer–Lambert equation stating $A = \varepsilon \times b \times C$ where A, ε, b, and C are absorptance of the solution, molar absorptivity, path length, and solution concentration, respectively. Since b and ε are constant, the parameter C is linearly proportional to the absorptance; thus, it can be obtained by measuring the parameter A. To do that, 50 ml of the MB solution (50 mg l^{-1}) and a 1 cm × 1 cm sample, as a photocatalyst, were placed in a quartz cell. A UV-lamp (Philips, 25 W) was used as an irradiation source during photocatalytic experiments. Prior to UV irradiation, in each experiment, the solution and the catalyst were left in the dark for 60 min (considered as a reference point) until adsorption/desorption equilibrium was reached. The solution was then irradiated by UV light (λ = 365 nm). A fixed quantity of the solution was removed every 20 min to measure the absorption and then the concentration. The absorptivity measurements were carried out at a fixed wavelength of 664 nm, because the maximum light absorption by the MB solutions occurs at this particular wavelength

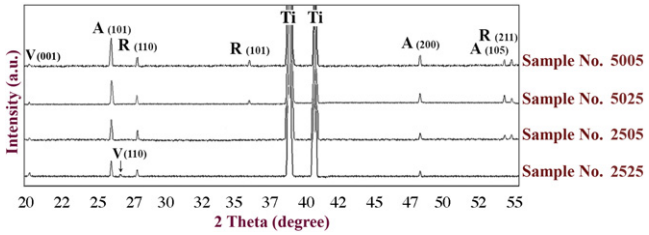

Fig. 1. XRD patterns and anatase fraction of V_2O_5–TiO_2 layers grown under different conditions.

[32]. The photoactivity of the synthesized layers under visible irradiation was also studied via a similar set of experiments under visible light with wavelengths ranging from 400 to 550 nm using a Xenon-lamp (Luminar Ace 210, Hayashi Takei Works).

3. Results and discussion

XRD patterns of the V_2O_5–TiO_2 layers are depicted in Fig. 1 where formation of the anatase, rutile, and vanadia phases are evident. Since the anatase phase of the TiO_2 layers is well known as a photoactive structure, its relative content (W_A) determines the degree of photocatalytic performance. Therefore, W_A was calculated using the formula $W_A = I_A/(I_A + I_R + I_V)$ where I_A, I_R, and I_V represent the normalized XRD-peak intensities of the anatase, rutile, and V_2O_5 phase, respectively (Fig. 2). Concerning accuracy of the XRD method as well as this formula, it is worthy to note that the values presented in Fig. 2 may not match the real amount of the anatase phase of the layers; however, they can be considered as a reliable criterion to only compare the phase structure of the samples, since any probable error is common for all samples and, hence, can be neglected. Comparing these results and the results obtained in our other works [27], it can be suggested that applying pulse current results in higher anatase fractions. The reason for such a difference is that the growing layer can cool down in the adjacent electrolyte when the current is off. Therefore, the anatase metastable phase does not transform to the rutile phase which is thermodynamically stable at all temperatures. In other words, the anatase to rutile phase transformation is suppressed. Duty cycle is defined as Φ = on-time/(on-time + off-time). Concerning this formula, on-time is longer at higher duty cycles and vice versa. The layer grows during on-times and cools down in the adjacent electrolyte during off-times. As a consequence, the growing layers are allowed to cool down more at low duty cycles, since the off-time is longer than on-time. Consequently, applying lower duty cycles

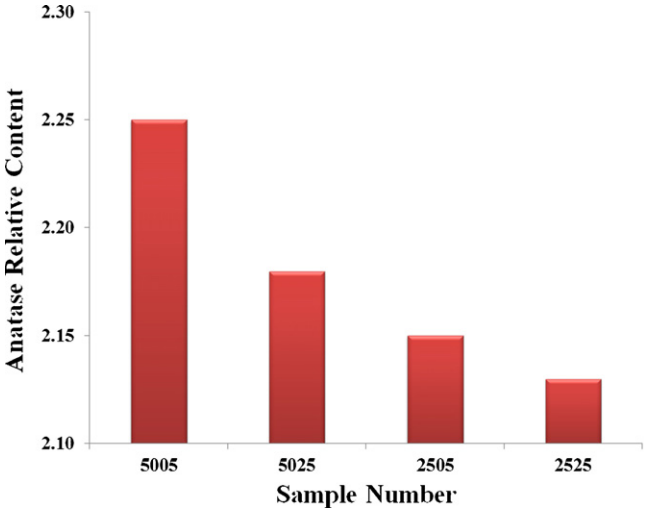

Fig. 2. Anatase relative contents for different samples.

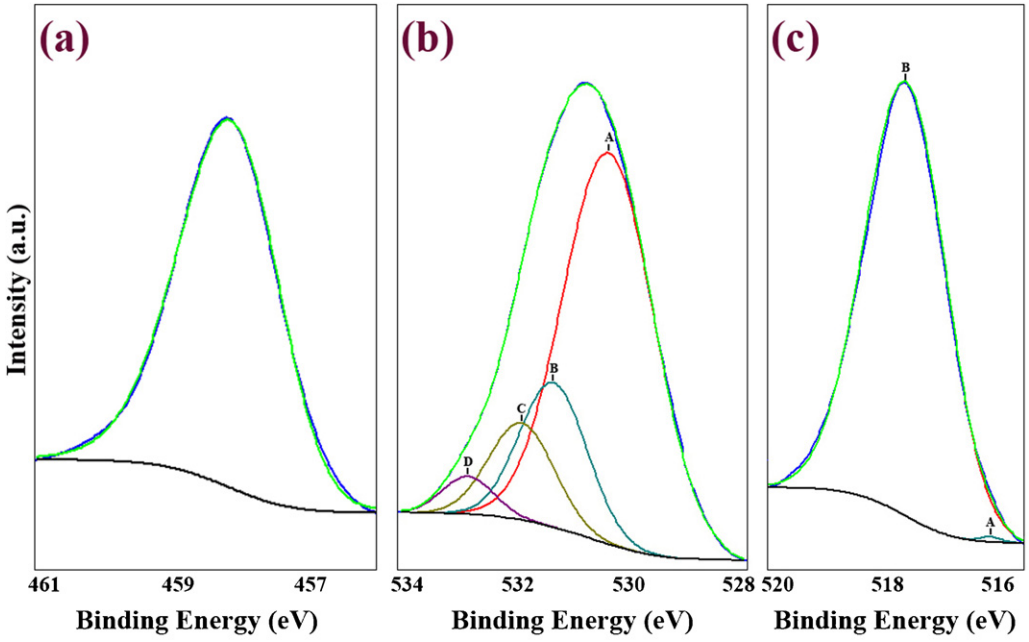

Fig. 3. XPS core level binding energy of: (a) Ti($2p_{3/2}$), (b) O(1s), and (c) V($2p_{3/2}$).

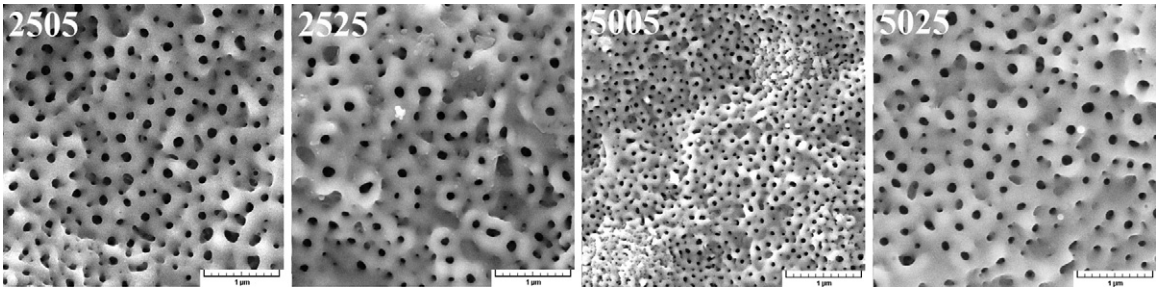

Fig. 4. SEM top-view of the grown V_2O_5–TiO_2 layers.

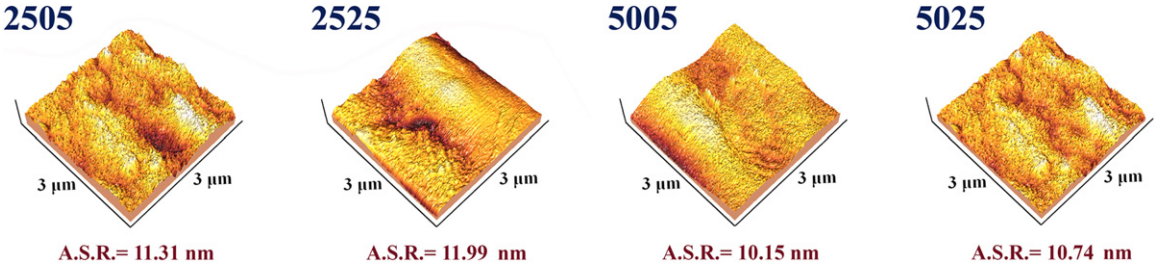

Fig. 5. AFM surface topography and average surface roughness of the grown V_2O_5–TiO_2 layers.

resulted in higher W_A. Another difference between phase structures of the V_2O_5–TiO_2 layers grown under direct and pulse currents is the amount of the vanadia phase dispersed in the titania matrix which decreased when pulse current was applied.

Since the layer grown under the frequency of 500 Hz and duty cycle of 5% had the highest anatase fraction, its surface chemical composition was further investigated by XPS technique whose results are presented in Fig. 3. It should be noted that all of the

Table 1
Summary of the growth conditions.

Sample no.	Electrolyte	Time (min)	Voltage (V)	Frequency (Hz)	Duty cycle (%)
2505	Na3PO4 (10 g l^{-1}) + NaVO3 (2 g l^{-1})	3	450	250	5
2525					25
5005				500	5
5025					25

binding energies were referenced to the C(1s) peak binding energy at 285 eV. Fig. 3a depicts the Ti($2p_{3/2}$) core level binding energy. The peak located at the binding energy of 458.6 eV asserts the existence of titanium in the form of Ti^{4+} state solely. Applying high voltages, which are much more than the electrochemical potentials of the titanium states, results in the formation of the oxides with highest states. According to Fig. 3b, the O(1s) peak were resolved into four distinct components. The peak A, located at 530.3 eV, is assigned to the crystal lattice oxygen (Ti–O and V–O), while the peaks B and C, at the binding energies of 531.4 and 531.9 eV, represent the oxygen in hydroxyl groups (O–H) and O^- with descending binding energy, respectively. Oxide free surfaces contacting with the atmosphere are always hydrated, i.e. contain water molecules and hydroxyl groups. Finally, the peak D, located at the binding energy of 533.0 eV, represents oxygen in the water molecules. Fig. 3c shows V($2p_{3/2}$) core level binding energy which was deconvoluted to two distinct peaks. The peaks A and B with binding energies of 516.1 and 517.7 eV correspond to V^{4+} and V^{5+}, respectively. As discussed earlier, oxides with the highest states form in the layers grown via micro arc oxidation process due to the high voltages applied. However, another phenomenon is prevailing as well. It has been suggested that V_2O_5 is stable at the temperatures below ~450 °C and transforms to other vanadium oxides such as VO_2 [33]. Applying high voltages results in increasing the temperature of the anode and the growing layer; as a consequence, V_2O_5 forms and, then, transforms to other vanadium oxides.

SEM surface morphology of the layers is shown in Fig. 4. Comparing these results and the SEM morphology of the vanadia–titania layers fabricated under direct current [27], it can be suggested that pores size decreases and finer structures are achieved when pulse current is applied. The reason is that the long-living electrical sparks which are responsible for formation of wide pores are to some extent eliminated [34]. Generation of such low energy sparks results in formation of smaller pores. Under this condition, a higher surface area is obtained and, thus, the photocatalytic efficiency is enhanced [29]. It is observed that the pore size decreases with frequency. Frequency is defined as the pulse number per second, or the reciprocal of the time for one cycle: $f = 1/t$ where f is the frequency (Hz) and t is the time of one cycle (s). The higher the frequency, the shorter the time of one cycle. For example, the time of one cycle is 0.0017 and 0.1 s for frequency of 600 and 10 Hz, respectively. The shorter time of one cycle means the more breakdowns per second and the less energy provided by one cycle leading to weaker electrical sparks. As a result, the electrical avalanches are shorter and weaker at high frequencies. In addition, it can be observed that the pore size increases with the duty cycle, because duration of sparks increases with this parameter. It is concluded that the finest pores formed under the frequency of 500 Hz and duty cycle of 5%.

Fig. 5 shows AFM surface topography of the layers where a rough surface is observed. Such a rough surface is usual for MAO-grown layers and increases the surface area. The average surface roughness numbers (A.S.R.) are also presented in this figure. The electron avalanches taking place on the anode surface result in local melting. After the sparks disappeared, the melted zones solidify in the adjacent electrolyte. This phenomenon makes the layers roughened. According to the statistical data analysis, it can be seen that the surface roughness decreases with the frequency and increases with the duty cycle.

In order to calculate the photocatalytic reactions rate constants (k), the quantity $\ln(C_o/C)$ versus irradiation time was plotted for different growth conditions. Straight lines, which are shown in Figs. 6 and 7, indicate that the degradation of MB is a first order process. The reactions rate constants (k) was calculated using the equation $\ln(C_o/C) = kt$ and the results are listed in Table 2. It is worthy to be noted that the layers were photoactive under both

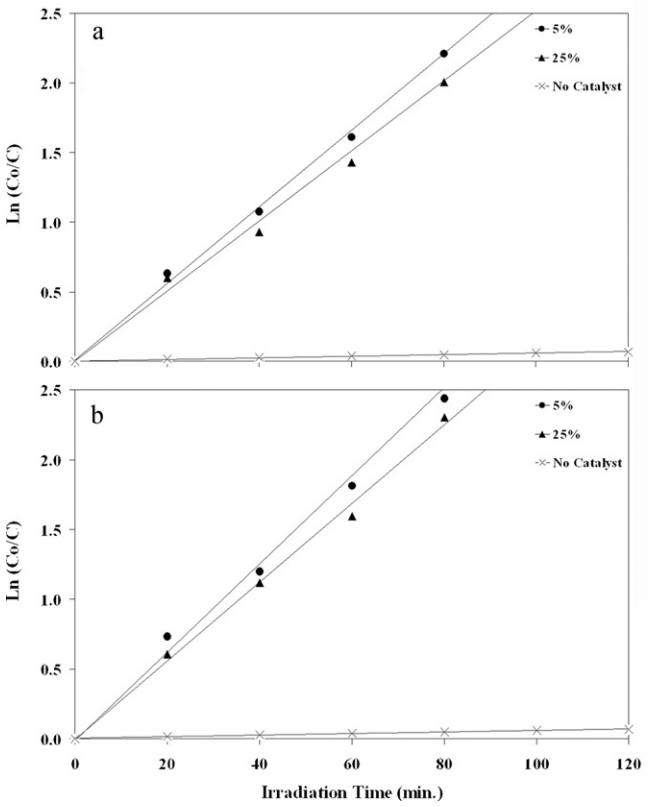

Fig. 6. $\ln(C_o/C)$ as a function of the ultraviolet irradiation for different synthesis conditions: (a) $f = 250$ Hz and (b) $f = 500$ Hz.

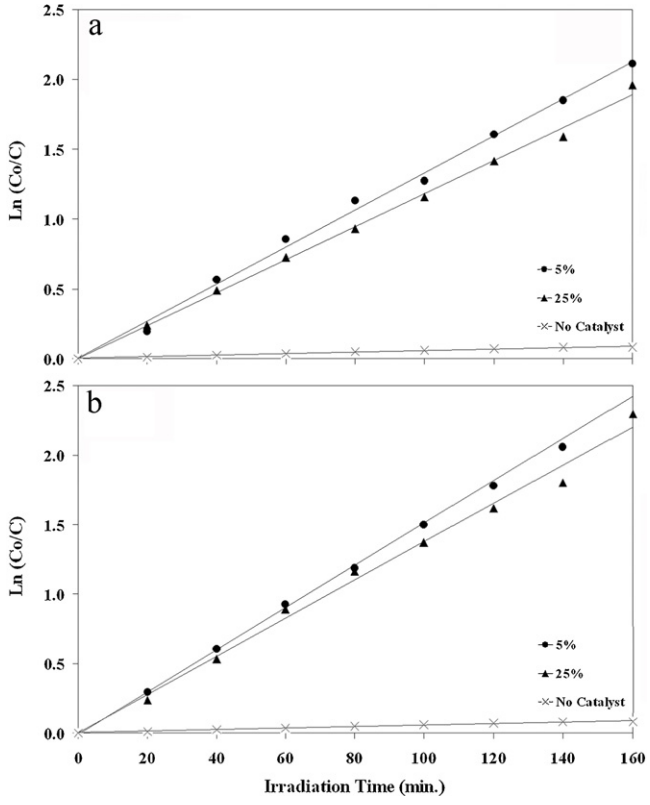

Fig. 7. $\ln(C_o/C)$ as a function of the visible irradiation for different synthesis conditions: (a) $f = 250$ Hz and (b) $f = 500$ Hz.

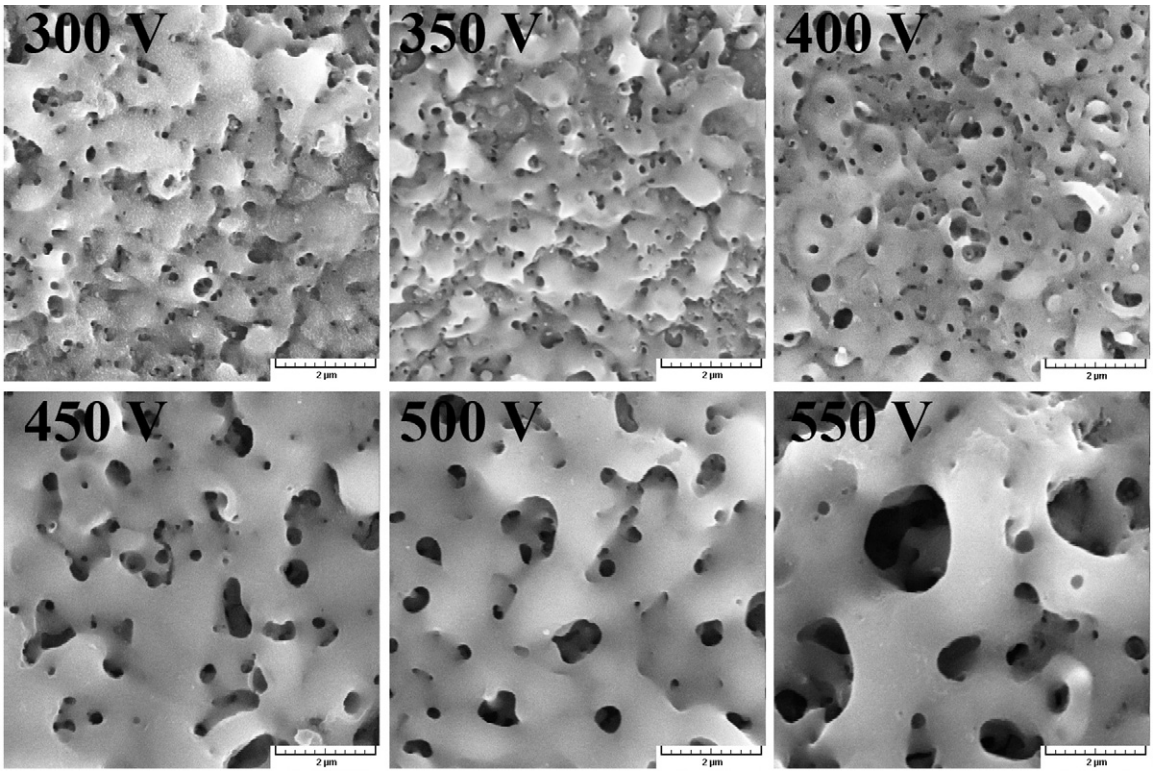

Fig. 8. SEM top-view of the vanadia–titania porous layers grown under DC mode [27].

ultra violet and visible irradiations due to their narrow band gap. Results of the optical studies on the layers can be found in our previous reports [27]. Comparing these results and those obtained in our previous study, it can be deduced that the vanadia–titania porous layers synthesized under pulse current are more photoactive than the layers grown under direct current. Three reasons are put forward for such a difference. The first reason is that the layers fabricated under pulse current had a finer pore size and, hence, higher surface area where the photocatalytic reactions take place. As shown in Fig. 8, larger pores were formed in the vanadia–titania layers fabricated under direct current. The reason is that the sparks taking place under DC mode have longer life. The second reason is the difference between phase structures. As elucidated earlier, applying pulse current instead of direct current resulted in higher anatase fractions. Regarding the fact that the growing layer cannot cool down in the adjacent electrolyte under direct current, the anatase–rutile phase transformation is encouraged in such layers resulting in lower anatase/rutile relative content, as shown in Figs. 9 and 10. Higher surface area and more anatase phase, which is the main photoactive phase of the layers, result in better photocatalytic performance. Another reason, which is also proposed, is the amount of the vanadia phase dispersed in the TiO_2 matrix. The amount of this phase is less in the layers synthesized under pulse current when compared to that of the layers fabricated under direct current [27]. It is well-known that only doped vanadium improves the photocatalytic activity of TiO_2. In contrast, the vanadia, which is dispersed in the matrix, adversely affects photocatalytic performance in high amounts, since photocatalytic activity of vanadia is significantly weaker than that of titania [35]. A comparison between the phase structure of the pulse-grown layers and those fabricated under the direct current [27] asserts that the diffraction angles of the anatase and the rutile phase for the DC and pulse grown layers are approximately equal. This shows that the amount of the doped vanadium does not change when the current type is altered. As a consequence, applying pulse current decreases the fraction of the dispersed vanadia, and, improves the photocatalytic efficiency. Moreover, the photocatalytic activity increases with the frequency. The reason is that the anatase fraction, affecting the photoactivity of the layers, increases with frequency, as explained before. Photocatalytic performance is also determined by surface area which was higher in the layers grown at the frequency of 500 Hz. It is clearly evident that the photocatalytic activity of the layers increases when the duty cycle decreases. The reason is the effect of this parameter on the surface area and the phase structure of the layers, as elucidated before. In conclusion,

Table 2
Photocatalytic reaction rate constants (k) for different growth conditions.

Illumination	Sample no.			
	2505	2525	5005	5025
Ultraviolet	0.0276	0.0252	0.0314	0.0281
Visible	0.0125	0.0116	0.0145	0.0135

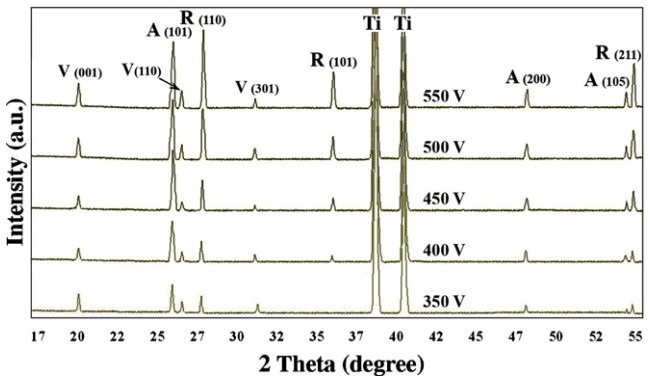

Fig. 9. XRD patterns of the vanadia–titania layers grown under DC mode [27].

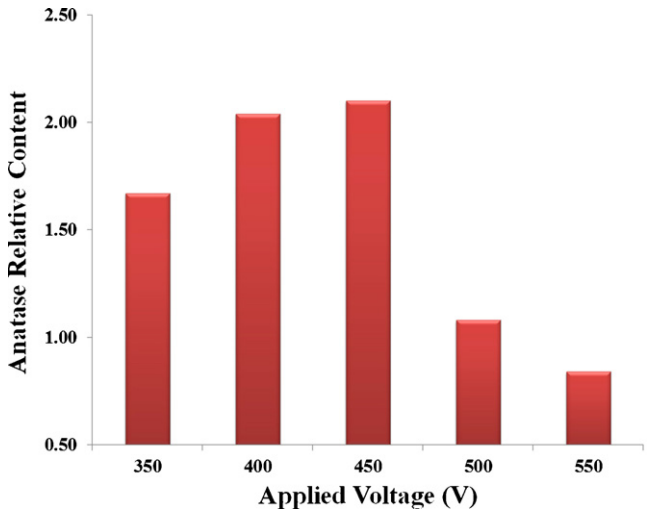

Fig. 10. Anatase relative content as a function of the voltage in the layers synthesized under DC mode [27].

the layer grown under the frequency of 500 Hz and duty cycle of 5% demonstrated the highest photocatalytic performance.

4. Conclusions

V_2O_5–TiO_2 porous layers with a rough surface were grown by micro arc oxidation process under pulse current. The layers had a fine porous structure where the pore size decreased with the frequency and increased with the duty cycle. They consisted of anatase, rutile, and vanadium oxides phases. The layers which were fabricated under the frequency and the duty cycle of 500 Hz and 5% had the highest anatase fraction. Photocatalytic activity of the layers was also examined by measuring the decomposition rate of methylene blue under both ultraviolet and visible photo irradiations. It was observed that the layers grown under pulse current were more photoactive as compared to the layers which were synthesized with applying direct current. It is finally suggested that a uniform porous structure with enhanced photocatalytic efficiency can be elaborated by changing the current type and altering the electric parameters.

Acknowledgement

The authors would like to thank all personnel in ceramic synthesis laboratory. The assistances of Mr. Rafi'ee for the XPS measurements and Mrs. Vaseghinia for the AFM images are also appreciated.

References

[1] A. Fujishima, X. Zhang, D.A. Tryk, Surf. Sci. Rep. 63 (2008) 515.
[2] C.C. Trapalis, P. Keivanidis, G. Kordas, M. Zaharescu, M. Crisan, A. Szatvanyi, M. Gartner, Thin Solid Films 433 (2003) 186.
[3] X. Zhang, H. Yang, F. Zhang, K.Y. Chan, Mater. Lett. 61 (2007) 2231.
[4] L. Li, C.Y. Liu, Y. Liu, Mater. Chem. Phys. 113 (2009) 551.
[5] Y. Liu, F. Xin, F. Wang, S. Luo, X. Yin, J. Alloys Compd. 498 (2010) 179–184.
[6] B. Wang, J. Yan, H. Cui, S. Du, J. Alloys Compd. (2011), doi:10.1016/j.jallcom.2011.02.008.
[7] H. Yan, H. Yang, J. Alloys Compd. 509 (2011) L26–L29.
[8] R.M. Mohamed, I.A. Mkhalid, J. Alloys Compd. 501 (2010) 301–306.
[9] E. Sahle-Demessie, V.G. Devulapelli, Appl. Catal. B: Environ. 84 (2008) 408.
[10] M.R. Bayati, F. Golestani-Fard, A.Z. Moshfegh, J. Appl. Catal. A: Gen. 382 (2010) 322.
[11] J. Wang, Z. Wang, H. Li, Y. Cui, Y. Du, J. Alloys Compd. 494 (2010) 372–377.
[12] F. Meng, F. Lu, J. Alloys Compd. 501 (2010) 154–158.
[13] J. Liu, Y. Fu, Q. Sun, J. Shen, Microporous Mesoporous Mater. 116 (2008) 614.
[14] H. Zhao, S. Bennici, J. Shen, A. Auroux, Appl. Catal. A 356 (2009) 121.
[15] N. Serpone, P. Maruthamuthu, P. Pichat, E. Pelizzetti, H. Hidaka, J. Photochem. Photobiol. A: Chem. 85 (1995) 247.
[16] H. Zhao, S. Bennici, J. Cai, J. Shen, A. Auroux, Catal. Today 152 (2010) 70.
[17] W. Zhou, Q. Liu, Z. Zhu, J. Zhang, J. Phys. D: Appl. Phys. 43 (2010) 035301.
[18] M.R. Bayati, F. Golestani-Fard, A.Z. Moshfegh, Mater. Chem. Phys. 124 (2010) 203.
[19] M.R. Bayati, A.Z. Moshfegh, F. Golestani-Fard, Mater. Lett. 64 (2010) 2215.
[20] M.R. Bayati, A.Z. Moshfegh, F. Golestani-Fard, Appl. Surf. Sci. 256 (2010) 2903.
[21] M.R. Bayati, A.Z. Moshfegh, F. Golestani-Fard, Appl. Catal. A: Gen. 389 (2010) 60.
[22] M.R. Bayati, H.R. Zargar, R. Molaei, F. Golestani-Fard, N. Zanganeh, A. Kajbafvala, Appl. Surf. Sci. 256 (2010) 3806.
[23] X. Jiang, Y. Wang, C. Pan, J. Alloys Compd. 509 (2011) L137.
[24] A.L. Yerokhin, X. Nie, A. Leyland, A. Matthews, S.J. Dowey, Surf. Coat. Technol. 122 (1999) 73.
[25] A.L. Yerokhin, V.V. Lyubimov, R.V. Ashitkof, Ceram. Int. 24 (1998) 1.
[26] A.L. Yerokhin, A.A. Voevodin, V.V. Lyubimov, J. Zabinski, M. Donley, Surf. Coat. Technol. 110 (1998) 140.
[27] M.R. Bayati, A.Z. Moshfegh, F. Golestani-Fard, Electrochim. Acta 55 (2010) 3093.
[28] M.R. Bayati, F. Golestani-Fard, A.Z. Moshfegh, Catal. Lett. 134 (2010) 162.
[29] M.R. Bayati, A.Z. Moshfegh, F. Golestani-Fard, Electrochim. Acta 55 (2010) 2760.
[30] M.R. Bayati, F. Golestani-Fard, A.Z. Moshfegh, Mater. Chem. Phys. 120 (2010) 582.
[31] M.R. Bayati, F. Golestani-Fard, A.Z. Moshfegh, Appl. Surf. Sci. 256 (2010) 4253.
[32] C. Yogi, K. Kojima, N. Wada, H. Tokumoto, T. Takai, T. Mizoguchi, H. Tamiaki, Thin Solid Films 516 (2008) 5881.
[33] J. Haber, Catal. Today 142 (2009) 100.
[34] A.L. Yerokhin, L.O. Snizhko, N.L. Gurevina, A. Leyland, A. Pilkington, A. Matthews, J. Phys. D: Appl. Phys. 36 (2003) 2110.
[35] M. Miyauchi, A. Nakajima, T. Watanabe, K. Hashimoto, Chem. Mater. 14 (2002) 2812.